2-μm emission performance of Tm^{3+}–Ho^{3+} co-doped tellurite glasses

Meng Wang (王 孟)[1,2], **Guonian Wang (汪国年)**[1*], **Lixia Yi (衣丽霞)**[1,2], **Shunguang Li (李顺光)**[1],
Lili Hu (胡丽丽)[1], **and Junjie Zhang (张军杰)**[1]

[1]*Key Laboratory of Material Science and Technology for High Power Lasers,*
Shanghai Institute of Optics and Fine Mechanics, Chinese Academy of Sciences, Shanghai 201800, China
[2]*Graduate School of Chinese Academy of Sciences, Beijing 100049, China*
*E-mail: wangwgn2942@mail.siom.ac.cn
Received March 30, 2009

The emission properties of 2-μm region fluorescence of Tm^{3+}–Ho^{3+} co-doped tellurite glasses are investigated. Introducing F$^-$ ions to the composition of tellurite glasses plays a positive effect on the 2-μm emission. A maximum intensity of 2-μm emission is achieved when 1.5-mol% Tm$_2$O$_3$ and 1-mol% Ho$_2$O$_3$ concentration are doped in the glasses. The emission cross section and gain coefficient of the ^{5}I$_8\rightarrow$^{5}I$_7$ transition of Ho^{3+} are calculated. The emission cross section has a maximum of 1.29×10^{-20} cm^2 at 2048 nm wavelength. The results indicate that Tm^{3+}–Ho^{3+} co-doped tellurite glasses are suitable for 2-μm application.

 OCIS codes: 160.5690, 160.4670, 300.6280, 160.2750.
 doi: 10.3788/COL20100801.0078.

Recently, 2-μm region laser emission is of great interest for its numerous potential applications, such as eye-safe laser lidar, remote sensing, and biomedical applications[1−4]. Tm^{3+} and Ho^{3+} ions play the most important part to achieve 2-μm emission because of the Tm^{3+}:^{3}F$_4 \rightarrow$ ^{3}H$_6$ and Ho^{3+}:^{5}I$_7 \rightarrow$ ^{5}I$_8$ transitions. Tm^{3+} ions can be pumped directly into the ^{3}H$_4$ level with an 800 nm source, and will show 1.8-μm emission. However, Ho^{3+} ions cannot directly absorb the pumped beam of 800 nm or other most common commercial laser diodes (LDs), due to the lack of an appropriate absorption band. Therefore, Ho^{3+} ions sensitized with Tm^{3+} ions are always considered. In a Tm^{3+}–Ho^{3+} co-doped glass, Tm^{3+}:^{3}H$_4$ level is populated by the 800 nm pump source and a quenching mechanism transfers energy to Ho^{3+}:^{5}I$_7$ level which then radiatively depopulates to the ground state of Ho^{3+}:^{5}I$_8$, giving rise to 2-μm emission[5].

Tellurite glass has several properties, which make it an interesting candidate to investigate the emission properties of rare earth ions for compact fiber laser applications. The main advantages of tellurite glasses over other laser glasses, such as silicates, are large rare earth ion solubility and extended infrared cut-off which are both comparable with fluoride hosts, and moderate phonon energy (600 – 800 cm^{-1}) which is significantly lower than both of germinate glasses (880 cm^{-1}) and silica glasses (1100 cm^{-1})[6]. Moreover, tellurite glasses are investigated extensively due to their high refractive index, high dielectric constant, good corrosion resistance, and thermal and chemical stability[7].

However, there is a very important disadvantage in tellurite glasses that it is difficult to remove OH$^-$ groups, which plays a detrimental effect on optical properties. Up to now, there are many reports about Tm^{3+}–Ho^{3+} co-doped tellurite glasses[8−10], nevertheless few researches about the effect of introducing F$^-$ on 2-μm emission by eliminating OH$^-$ groups in tellurite glasses are operated. This letter aims to investigate the difference of 2-μm emission with introducing F$^-$ and the optimization of rare earth ions doped concentration in tellurite glasses.

The compositions of tellurite glasses are shown in Table 1. All started materials are of analytical grade. Well-mixed batches were melted in a platinum crucible at 750–900 °C for 30 min while being bubbled with dry oxygen gas; then the liquids were cast into graphite moulds. The obtained glasses were annealed for several hours at the glass transition temperatures before they were cooled to room temperature at a rate of 15 °C/h. Finally, the samples for optical and spectroscopic properties measurements were cut and polished with the size of 15$\times$10$\times$1 (mm).

Table 1. Composition of the Tellurite Glasses

Code	Glass composition(mol%)
TF1	70TeO$_2$-**10ZnO-10ZnF$_2$**-4.5PbO-3Nb$_2$O$_5$-1Ho$_2$O$_3$-1.5Tm$_2$O$_3$
TF2	70TeO$_2$-**5ZnO-15ZnF$_2$**-4.5PbO-3Nb$_2$O$_5$-1Ho$_2$O$_3$-1.5Tm$_2$O$_3$
TF3	70TeO$_2$-**0ZnO-20ZnF$_2$**-4.5PbO-3Nb$_2$O$_5$-1Ho$_2$O$_3$-1.5Tm$_2$O$_3$
TFH0	70TeO$_2$-19ZnF$_2$-4PbO-3Nb$_2$O$_5$-**3La$_2$O$_3$**-1Ho$_2$O$_3$
TFH1	70TeO$_2$-19ZnF$_2$-4PbO-3Nb$_2$O$_5$-**2.5La$_2$O$_3$**-1Ho$_2$O$_3$-**0.5Tm$_2$O$_3$**
TFH2	70TeO$_2$-19ZnF$_2$-4PbO-3Nb$_2$O$_5$-**2La$_2$O$_3$**-1Ho$_2$O$_3$-**1Tm$_2$O$_3$**
TFH3	70TeO$_2$-19ZnF$_2$-4PbO-3Nb$_2$O$_5$-**1.5La$_2$O$_3$**-1Ho$_2$O$_3$-**1.5Tm$_2$O$_3$**
TFH4	70TeO$_2$-19ZnF$_2$-4PbO-3Nb$_2$O$_5$-**1La$_2$O$_3$**-1Ho$_2$O$_3$-**2Tm$_2$O$_3$**
TFH5	70TeO$_2$-19ZnF$_2$-4PbO-3Nb$_2$O$_5$-**0La$_2$O$_3$**-1Ho$_2$O$_3$-**3Tm$_2$O$_3$**

The absorption spectra were recorded with a Perkin-Elmer Lambda 900 UV/VIS/NIR spectrophotometer in the range of 350 – 2200 nm. The emission spectra were measured with a Triax 550 type spectrometer (Jobin-Yvon., France) upon excitation of 800 nm LD in the range of 1.6 – 2.2 μm. All the measurements were performed at room temperature.

Figure 1 presents the emission spectra of TF1–TF3 samples in which ZnO is substituted by ZnF_2 in turn. It can be found the intense double peak at 2 μm corresponding to $Ho^{3+}:^5I_7 \rightarrow {}^5I_8$ transition and a little feeble peak at 1.8-μm corresponding to $Tm^{3+}:^3F_4 \rightarrow {}^3H_6$ transition. The spectra show the 2-μm emission intensity increases with the decreased ZnO content, and when ZnO is completely substituted by ZnF_2 in TF3 sample, the intensity becomes largest. The inset in Fig. 1 illustrates how the peak intensity increases with the ZnF_2 content. It indicates that the introduction of F^- into tellurite glasses can affect 2-μm emission actively. As is known, a considerably high amount of OH^- groups is present in tellurite glasses while the glasses are melted in air. OH^- plays a detrimental effect by quenching the emission of rare earth ions[11]. However, F^- ions and OH^- groups are isoelectronic with a similar ionic size, so that the OH^- groups can be easily replaced by F^- ions by the equation $OH^- + F^- \rightarrow HF + O^{2-}$. Therefore, with F^- ions introduced in tellurite glasses, 2-μm emission becomes intense. From the results, the composition of tellurite glass with high substituting ZnF_2 content should be chosen.

In Fig. 2, the absorption spectra of Ho^{3+} doped TFH0 and Tm^{3+}–Ho^{3+} co-doped TFH1-TFH5 samples over the wavelength region of 350 – 2200 nm are shown. The shapes of the spectra for TFH1–TFH5 samples are similar, with no shift in the wavelength of the absorption peak. Several important absorption bands of Tm^{3+} and Ho^{3+} are indicated in the spectra, and the absorption intensities of Tm^{3+} are in proportion to the doped mole fraction of Tm^{3+}, while the intensities of Ho^{3+} are almost the same. The absorption spectrum of Ho^{3+} doped TFH0 is measured to calculate the absorption cross section. Identified from the absorption spectra, the energy levels of Tm^{3+} and Ho^{3+} are illustrated in Fig. 3. Tm^{3+} ions can absorb 800-nm pumping beam, transfer energy to Ho^{3+} ions, and then emit 2-μm fluorescence. The pumped schemes and energy transfer processes have
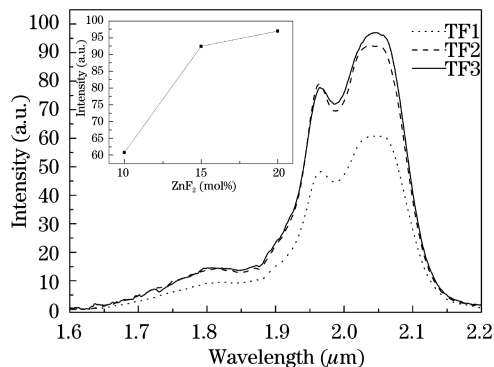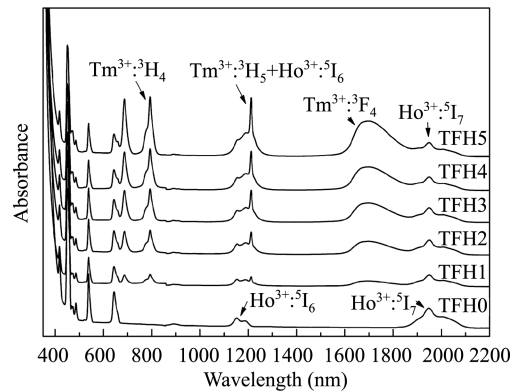

Fig. 2. Absorption spectra of Ho^{3+} doped TFH0 and Tm^{3+}–Ho^{3+} co-doped TFH1–TFH5 samples.
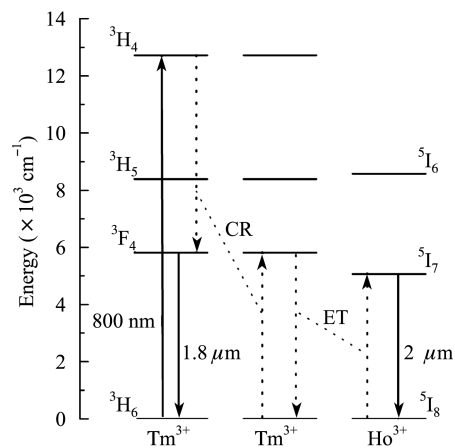

Fig. 3. Energy level diagrams of Tm^{3+} and Ho^{3+} in tellurite glass (CR: cross-relaxation, ET: energy transfer).
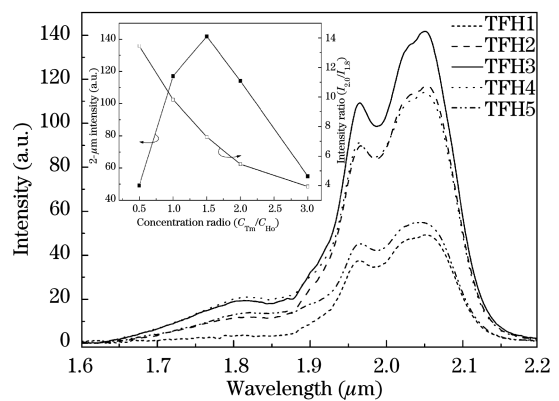

Fig. 4. Emission spectra of Tm^{3+}–Ho^{3+} co-doped TFH1–TFH5 samples pumped by 800 nm. Inset shows the relationship between the 2-μm emission intensity and C_{Tm}/C_{Ho}, and the peak intensity ration of 2-μm emission with respect to 1.8-μm emission $I_{2.0}/I_{1.8}$.

been discussed in many researches[5,12].

Figure 4 shows the emission spectra of TFH1–TFH5 samples, with the radio of Tm_2O_3 concentration with respect to Ho_2O_3 concentration (C_{Tm}/C_{Ho}) varying from 0.5 to 3. The intensities of two emission peaks at 1.8 and 2 μm are changing by varying C_{Tm}/C_{Ho}. Emission at 2 μm, firstly increases, up to a maximum for C_{Tm}/C_{Ho} at 1.5, and then decreases. Similarly, emission at 1.8 μm is also found to increase firstly, and then decreases, but

Fig. 1. Emission spectra of Tm^{3+}–Ho^{3+} co-doped TF1–TF3 samples pumped by 800 nm. Inset shows the peak intensity with the Z_nF_2 content varying.

the maximum emission is recorded for C_{Tm}/C_{Ho} at 2. The inset of Fig. 4 shows the relationship between the 2-μm emission intensity and C_{Tm}/C_{Ho}. The largest intensity reaches to 141.8 when the C_{Tm}/C_{Ho} is 1.5 in the TFH3 sample. On the one hand, these suggest the presence of energy transferred from Tm^{3+} to Ho^{3+}, as shown in Fig. 3. According to the researches of Peng[13], the energy transferred from $Tm^{3+}:^3F_4$ to $Ho^{3+}:^5I_7$ is very efficient when the C_{Tm}/C_{Ho} is relatively small, and the energy back-transferred from $Ho^{3+}:^5I_7$ to $Tm^{3+}:^3F_4$ is low. This is the reason that 2 μm emission intensity increases before C_{Tm}/C_{Ho} exceeding 1.5. On the other hand, when the C_{Tm}/C_{Ho} is larger than 1.5, the energy back-transferred from Ho^{3+} to Tm^{3+} enhances, meanwhile the cross-relaxation of $Tm^{3+}:^3H_4+^3H_6 \rightarrow {}^3F_4+^3F_4$ (Fig. 3) strengthens, leading to the increase of 1.8-μm emission and decrease of 2-μm emission. Finally, while C_{Tm}/C_{Ho} reaches to 3, 1.8 and 2-μm emission intensities both weaken, resulting from concentration quenching. Another following elaboration of the results is also carried out by reporting the peak intensity ratio of 2-μm emission with respect to 1.8-μm emission ($I_{2.0}/I_{1.8}$). The obtained data are also reported in the inset of Fig. 4. The maximum for C_{Tm}/C_{Ho} at 1.5 is clear, and $I_{2.0}/I_{1.8}$ decreases monotonously with C_{Tm}/C_{Ho} increasing. This indicates that, when C_{Tm}/C_{Ho} increases, it causes the negative change in $I_{2.0}/I_{1.8}$. However, the $I_{2.0}/I_{1.8}$ of TFH3 sample is still 7.3, meaning that the intensity of 2-μm emission is 7.3 times as large as 1.8-μm emission, where the strongest 2-μm emission is achieved; consequently it is large enough to be accepted. In a word, from the application point of view the emission spectra show that TFH3 sample exhibits a large emission spectrum from 1900 to 2100 nm and appropriate intensity radio of 2-μm emission to 1.8-μm emission, therefore it is an excellent candidate for tunable laser source.

Figure 5 presents the absorption cross section and emission cross section of $Ho^{3+}:^5I_8 \rightarrow {}^5I_7$ transition at the 2-μm region. The absorption cross section (σ_a) can be deduced from the absorption spectra using

$$\sigma_a(\lambda) = \frac{2.303 \log(I_0/I)}{Nl}, \qquad (1)$$

where N is the concentration of Ho^{3+}, l is the thickness of the samples, and $\log(I_0/I)$ is the absorptivity from absorption spectra, respectively. The McCumber formula [14] is used to calculate the emission cross section
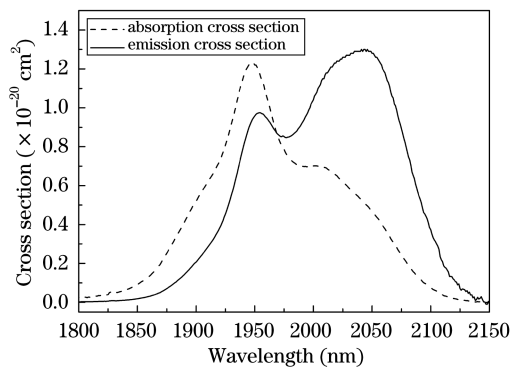
(σ_e) from the absorption section:

$$\sigma_e(\lambda) = \sigma_a(\lambda) \times \frac{Z_l}{Z_u} \times \exp\left[\frac{hc}{kT} \times \left(\frac{1}{\lambda_{ZL}} - \frac{1}{\lambda}\right)\right], \qquad (2)$$

where Z_l and Z_u are the partition functions respectively for the lower and upper levels involved in the considered optical transition, T is the temperature (here is the room temperature), k is the Boltzmann constant, and λ_{ZL} is the wavelength for the transition between the lower Stark sublevels of the emitting multiplets and those of the receiving multiplets. As shown in Fig. 5, the emission cross section of $Ho^{3+}:^5I_8 \rightarrow {}^5I_7$ transition has a maximum of 1.29×10^{-20} cm^2 at 2048 nm. This value is about two times as large as that in fluoride glass[5], and also a little larger than that of Te-W-Zn glass[15], but smaller than the value of Ge-Ga-S glass[16].

To calculate the gain coefficient, the reabsorption of the signal beam by the ground-state absorption should be considered since the terminal $^5I_8$ level of the 2-μm emission is the ground state of Ho^{3+}. Therefore, the gain coefficient can be calculated by[17]

$$G(\lambda) = n(^5I_7)\sigma_e(\lambda) - n(^5I_8)\sigma_a(\lambda), \qquad (3)$$

where $n(^5I_7)$ and $n(^5I_8)$ are the electron population densities of the $^5I_7$ and $^5I_8$ levels in Ho^{3+}, respectively. Assuming electrons in Ho^{3+} are only in either the $^5I_7$ or $^5I_8$ state, Eq. (3) can be simplified to

$$G(\lambda) = N\left[p\sigma_e(\lambda) - (1-p)\sigma_a(\lambda)\right], \qquad (4)$$

$$p = \frac{n(^5I_7)}{N}, \qquad (5)$$

where N is the total concentration of Ho^{3+}. By assuming several different p values, the values of $G(\lambda)$ can be calculated as shown in Fig. 6. As the value of p decreases, the peak wavelength at which the maximum values of $G(\lambda)$ occur shifts to longer wavelengths. This variation is a typical feature of the quasi-three-level laser system[17].

In conclusion, the 2-μm emission properties of Tm^{3+}–Ho^{3+} co-doped tellurite glasses are investigated. In tellurite glasses, the introduced F^- plays a positive impact for 2-μm emission. Therefore, the composition with high
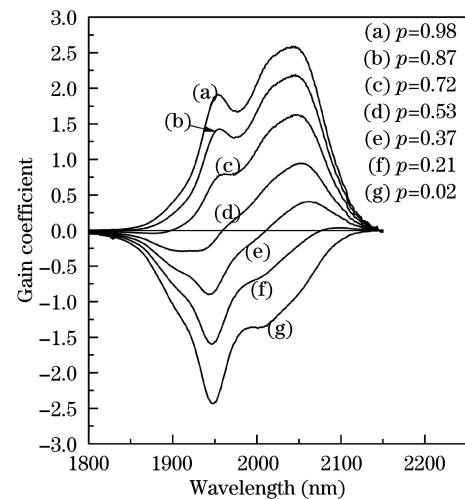

Fig. 5. Absorption cross section and emission cross section of $Ho^{3+}:^5I_8 \rightarrow {}^5I_7$ transition at 2-μm region.

Fig. 6. Gain spectra of Ho^{3+} at 2-μm region.

substituting ZnF_2 content is chosen. A maximum 2-μm emission intensity for 1.5-mol% Tm_2O_3 concentration and 1-mol% Ho_2O_3 concentration doped is obtained, when the emission properties of different rare earth ions doped tellurite glasses are investigated. In addition, the emission cross section, absorption cross section, and gain coefficient of $Ho^{3+}{:}^5I_8 \rightarrow {}^5I_7$ transition are calculated. The emission cross section of this tellurite glass is $1.29{\times}10^{-20}$ cm^2 at 2048-nm wavelength with a typical gain of the three-level laser system. Therefore this Tm^{3+}–Ho^{3+} co-doped tellurite glass is an excellent candidate for 2-μm region application.

References

1. K. Scholle, E. Heumann, and G. Huber, Laser Phys. Lett. **1,** 285 (2004).
2. S. Agger, J. H. Povlsen, and P. Varming, Opt. Lett. **29,** 1503 (2004).
3. Y. Li, Y. Ju, Y. Urata, and Y. Wang, Chin. Opt. Lett. **5,** 351 (2007).
4. Y. Tang, Y. Yang, X. Cheng, and J. Xu, Chin. Opt. Lett. **6,** 44 (2008).
5. X. Zou and H. Toratani, J. Non-Cryst. Solids **195,** 113 (1996).
6. L. Huang, S. Shen, and A. Jha, J. Non-Cryst. Solids **345 & 346,** 349 (2004).
7. G. Wang, S. Dai, J. Zhang, L. Wen, J. Yang, and Z. Jiang, Spectrochim. Acta Part A **64,** 349 (2006).
8. B. Richards, S. Shen, A. Jha, Y. Tsang, and D. Binks, Opt. Express **15,** 6546 (2007).
9. B. D. O. Richards, S. Shen, and A. Jha, Proc. SPIE **5984,** 598407 (2005).
10. G. Chen, Q. Zhang, G. Yang, and Z. Jiang, J. Fluoresc. **17,** 301 (2007).
11. D. Milanese, M. Vota, Q. Chen, J. Xing, G. Liao, H. Gebavi, M. Ferraris, N. Coluccelli, and S. Taccheo, J. Non-Cryst. Solids **354,** 1955 (2008).
12. D. Shi, Q. Zhang, G. Yang, and Z. Jiang, J. Non-Cryst. Solids **353,** 1508 (2007).
13. B. Peng and T. Izumitani, Opt. Mater. **4,** 797 (1995).
14. D. E. McCumber, Phys. Rev. **136,** A954 (1964).
15. G. Chen, Q. Zhang, G. Yang, Z. Yang, and Z. Jiang, Acta Phys. Sin. (in Chinese) **56,** 4200 (2007).
16. Y. S. Kim, W. Y. Cho, Y. B. Shin, and J. Heo, J. Non-Cryst. Solids **203,** 176 (1996).
17. Y. B. Shin, H. T. Lim, Y. G. Choi, Y. S. Kim, and J. Heo, J. Am. Ceram. Soc. **83,** 787 (2000).